Energetics and formation mechanism of borders between hexagonal boron nitride and graphene

doi: 10.7567/APEX.11.065201

Energetics and formation mechanism of borders between h-BN and graphene

Hisaki Sawahata[1*], Ayaka Yamanaka[2†], Mina Maruyama[1‡], and Susumu Okada[1§]

[1]*Graduate School of Pure and Applied Sciences, University of Tsukuba, 1-1-1 Tennodai, Tsukuba, Ibaraki 305-8571, Japan*

[2]*Research Organization for Information Science and Technology (RIST), 1-18-6 Hamamatsucho, Minato-ku, Tokyo 105-0013, Japan*

We studied the energetics of two-dimensional heterostructures consisting of h-BN and graphene with respect to the border structure and heterobond species using the density functional theory. A BC heterobond is energetically preferable at the border between h-BN and graphene. We also found the polarization at the zigzag border increase the total energy of the heterostructures. Competition between the bond formation energy and the polarization energy leads to the chiral borders where BC heterobonds are dominant. By taking the formation process of the heterostructures into account, the zigzag border with BC heterobond is preferentially synthesized from graphene edges and under the hydrogen rich condition.

A layered structure comprising a hexagonal covalent network endows graphene with unusual electronic structure which is characterized by pairs of linear dispersion bands at the Fermi level and six corners of the Brillouin zone causing unusual physical properties under appropriate conditions.[1–6)] The electronic structure of graphene derivatives are sensitive to their dimensionality, size, and shapes, which are determined by the boundary condition imposed on the hexagonal network. Tubular forms of graphene (CNTs) are either metals or semiconductors, depending on their atomic arrangement along their circumference.[7–9)] By imposing an open boundary condition, graphene nanoribbons exhibit similar variations in their electronic structure to the CNTs. The graphene nanoribbons with armchair or near armchair edges possess metallic and semiconducting electronic structures depending on their width and edge shape. The band gap of the nanoribbons with armchair and near armchair edges is inversely proportional to the ribbon width.[10–13)] In contrast, the graphene nanoribbons with zigzag and near zigzag

*E-mail: hsawahata@comas.frsc.tsukuba.ac.jp
†E-mail: yamanaka@rist.or.jp
‡E-mail: mmaruyama@comas.frsc.tsukuba.ac.jp
§E-mail: sokada@comas.frsc.tsukuba.ac.jp

edges possess the peculiar electronic structure at the Fermi level, which is absent in the electronic structure of the bulk graphene. A pair of π states exhibits flat band nature around the Brillouin zone boundary with an edge localized nature, leading to the spin polarization around their edges.

In addition to the nanostructure of graphene, graphene can form in-plane heterogeneous structures with boron (B) and nitrogen (N) atoms, because these elements possess the similar ionic radii to that of C atom. BC_3 and BC_2N compounds with graphitic networks have been synthesized, and their physical properties have been intensively studied.[14–20] In such compounds, the π network of graphene is segmented by the foreign B and N atoms so that their electronic structures strongly depend on the atomic arrangements of consistent elements in a hexagonal network. Furthermore, recent advances in the synthesis techniques of two-dimensional materials with atom thickness have realized a bulk grain boundary between graphene and h-BN[21–27] because of the small lattice mismatch between them. Furthermore, the experiment revealed that the BC heterobonds are preferentially generated at the zigzag border between graphene and h-BN.[28] From the theoretical studies, it has been predicted that the h-BN domain perfectly terminates the π states of graphene at the border, leading to spin polarization induced by the border-localized states at the zigzag border of C and B/N that possess similar characteristics to the edge state of graphene with zigzag edges.[29–32]

Despite the experiments and theories have been elucidating fundamental aspects of the in-plane heterostructures consisting of graphene and h-BN, their energetics, detail electronic structures, and formation mechanism are still unclear. In particular, the energetics and formation mechanism of the heterostructures with regard to the border structure are highly demanded for their synthesis and practical applications. Thus, in this work, we aim to investigate the energetics and formation mechanism of in-plane heterostructures of graphene and h-BN with respect to their border shapes and hetero-bonds, using the density functional theory (DFT) with the generalized gradient approximation (GGA).

All calculations were performed in the framework of DFT[33,34] using the Simulation Tool for Atom TEchnology (STATE) package.[35] To calculate the exchange-correlation energy among the interacting electrons, we used the GGA with the functional form of Perdew-Burke-Ernzerhof.[36,37] Ultrasoft pseudopotentials generated using the Vanderbilt scheme were employed to describe the interaction between electrons and nuclei.[38] The valence wave functions and deficit charge density were expanded in terms of the

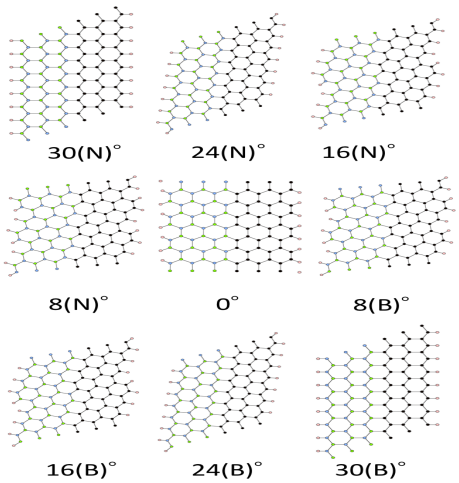

Fig. 1. Optimized geometries of nanoribbons consisting of h-BN and graphene nanostrips with the BC zigzag (30(B)°), BC dominant chiral (24(B), 16(B), and 8(B)°), nonpolar armchair (0°), NC dominant chiral (24(N), 16(N), and 8(N)°), and NC zigzag (30(N)°) borders. Green, black, blue, and pink circles denote B, C, N, and H, respectively.

plane-wave basis set with cutoff energies of 25 and 225 Ry, respectively. Integration over the one-dimensional Brillouin zone was carried out using equidistant k-point sampling in which 4 k-points were taken along ribbon direction, which give sufficient convergence in both electronic and geometric structures of graphene and h-BN nanostructures.[39,40] The atomic structure of BNC heterostructures were optimized until the force acting on each atoms were less than 5 mRy/Å under fixed lateral lattice parameters which correspond with the length calculated by the experimental C-C bond length of bulk graphene (1.42 Å).

To simulate the heterostructures consisting of h-BN and graphene, we consider the nanoribbons with hydrogenated edges, which consist of h-BN and graphene nanostrips with zigzag, chiral, and armchair edges. According to the choice of the nanostrips, the heterostructures contains the BC zigzag (30(B)°), BC dominant chiral (24(B), 16(B), and 8(B)°), nonpolar armchair (0°), NC dominant chiral (24(N), 16(N), and 8(N)°), and NC zigzag (30(N)°) borders (Fig. 1). The effective screening medium (ESM) method was adopted to investigate the energetics and formation mechanism of nanoribbons containing borders between h-BN and graphene, to exclude the unintentional dipole interaction with adjacent nanoribbons arising from the work function difference between graphene and h-BN strips.[41] An open boundary condition is imposed at the cell bound-

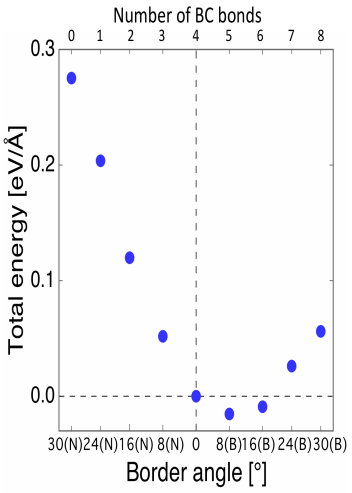

Fig. 2. The total energy per length of the heterostructures consisting of h-BN and graphene nanostrips as a function of the border angle or the number of BC heterobonds. Border angles of 30(N) and 30(B)° correspond with the zigzag borders consisting only of NC and BC bonds, respectively, and that of 0 ° corresponds with the armchair border.

aries described by a relative permittivity of 1 with the vacuum spacing of 7.5 Å from the edges of the nanoribbons.

Figure 2 shows the total energy of heterostructures consisting of h-BN and graphene nanostrips with respect to their border angles from 30(N) to 30(B)°.

$$E = \frac{E_{\mathrm{BNC}} - N_{\mathrm{BN}}\mu_{\mathrm{BN}} - N_{\mathrm{C}}\mu_{\mathrm{C}} - N_{\mathrm{H}}\mu_{\mathrm{H}}}{N_{\mathrm{BN}} + N_{\mathrm{C}}}$$

where E_{BNC}, μ_{C}, μ_{BN}, μ_{H}, N_{C}, N_{BN}, and N_{H} denote an energy of the heterostructure of h-BN and graphene strips, a chemical potential of C atom evaluated by graphene, a chemical potential of a BN pair evaluated by the total energy of a h-BN sheet, a chemical potential of H evaluated by the total energy of H_2 molecule, the number of C atoms, the number of BN pairs, and the number of H atoms, respectively. The energy has a minimum at the border angle of 8(B)° where the border possess the chiral shape consisting of 5 BC and 3 NC heterobonds. The energy increase with increase and decrease of the border angles or the number of BC heterobonds. According to the asymmetric energy profile, the energy of the zigzag border consisting only of BC heterobonds is lower by 0.22 eV per length than that of the zigzag border consisting only of NC heterobonds. The fact implies that the heterostructures prefer the border comprising BC heterobonds, although the total energy has the smallest value at the border angle of 8(B)°. On the other hand, the polarity at the border may increase

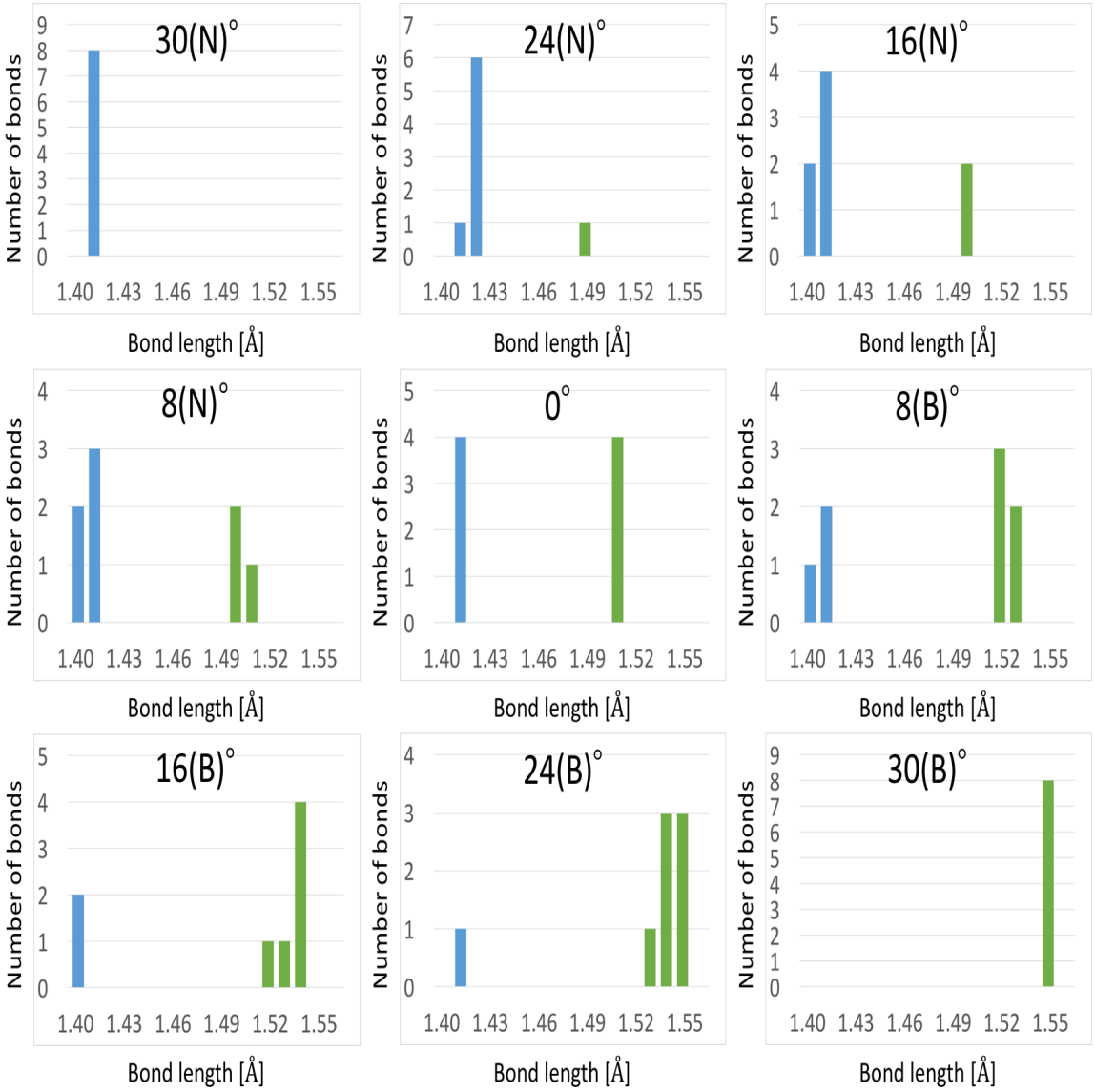

Fig. 3. Distribution of the bond length at the border of the heterostructures consisting of h-BN and graphene strips. Green and blue bars indicate the distribution of the bond length of BC and NC heterobonds, respectivity. Border angles of θ(N) and θ(B)° indicate the border angle θ consisting mainly of NC and BC heterobonds, respectively. The $\theta = 0$ ° corresponds with the armchair border.

with the electrostatic energy of the heterostructures with increasing the border angles from 0° corresponding with the armchair border. Thus, the competition between the heterobond energy and the polar energy at the border leads to the asymmetric energy profile with respect to the border angles.

Figure 3 shows the distribution of the bond length at the border of the heterostructures consisting of h-BN and graphene nanostrips. The optimized length of the heter-

obonds are 1.41 and 1.51 Å for NC and BC heterobonds, respectively, for the armchair border. With increasing the border angle or the number of BC heterobonds, the BC heterobond is gradually elongated up to the length of 1.55 Å at the zigzag border consisting only of BC heterobonds. The optimum length of the BC heterobond at the zigzag border well agree with the other BC heterobonds in various complexes comprising B and sp^2 C atoms, indicating that the zigzag border with BC heterobonds has remarkable stability. On the other hand, for the NC bond rich border, bond length of the BC heterobond further decrease with decreasing the number of the BC bonds, causing the increase of the energy of the heterostructures, with respect to the BC bond length. Therefore, the BC bond is preferential heterobonds in the heterostructures in the view of the bonding geometries.

Next, we investigate the formation energy of the border between graphene and h-BN for providing the microscopic mechanism of the preferential formation of BC heterobonds at the zigzag edges of graphene experimentally observed.[28] Figures 4(a) and 4(b) show the optimized structures of the zigzag edges of graphene ribbons adsorbing the BN pairs with BC and NC heterobonds, respectively. The adsorption energy of a BN pair with the BC heterobond is larger by 0.42 eV/bond than that with the NC heterobond. Therefore, for the zigzag edge of graphene, h-BN grows with the formation of BC heterobonds [Fig. 4(c)]. At the graphene edges with chiral and armchair shapes, armchair portions of the edges lead to the NN and BB bonds under the preferential formation of BC heterobonds at the graphene edges, so that the formation of h-BN from the graphene with the armchair and chiral edges is prohibited in the early stages of BN adsorption [Fig. 4(d)].

Finally, we investigated the formation energy of borders between h-BN and graphene nanostrips by connecting their edges. The border formation energy ΔE is evaluated by the reactions

$$\text{h-BN strip} + \text{Gra. strip} \rightarrow \text{h-BN/Gra} + \Delta E$$

for ultrahigh vacuum condition where the strips possess clean edges, and

$$\text{h-BN strip-H} + \text{Gra. strip-H} \rightarrow \text{h-BN/Gra} + 8 \times \text{H}_2 + \Delta E$$

for the hydrogen rich condition where the edges of the strips are terminated by H atoms. Figure 5(a) shows the border formation energy in the reaction of the hydrogenated strips. The border energy monotonically decrease with increasing the number

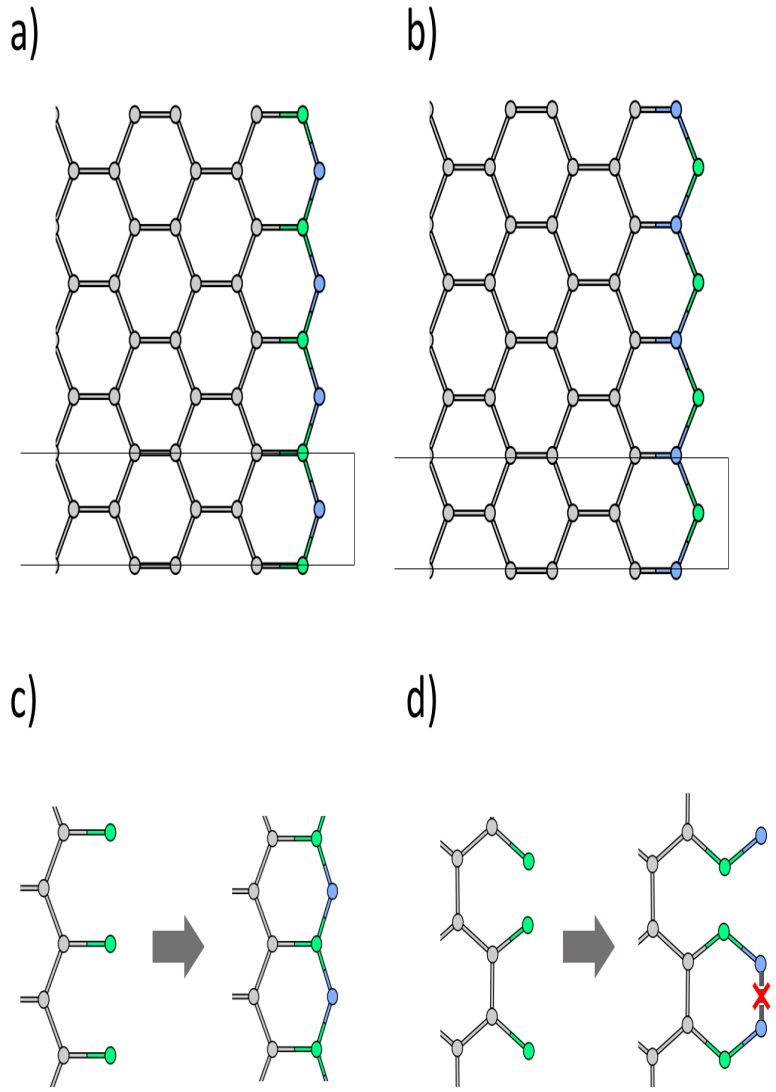

Fig. 4. Optimized structures of graphene with zigzag edges adsorbing a BN with (a) BC and (b) NC heterobonds. Black lines indicate the unit cell of the structures. Schematic views of formation of the first and second formation steps of h-BN at (c) the zigzag and (d) armchair edges of graphene. Green, gray, and blue circles indicate B, C, and N atoms, respectively.

of BC heterobond at the border. Furthermore, the reaction is exothermic for the zigzag border consisting only of BC heterobonds. Therefore, under the hydrogen rich condition, the heterostructure of h-BN and graphene possesses the zigzag border with BC heterobonds. In contrast, under the ultra-high vacuum condition, the reactions are all exothermic because of the formation of covalent bond between h-BN and graphene strips, which saturate the dangling bonds of them [Fig. 5(b)]. Furthermore, the zigzag

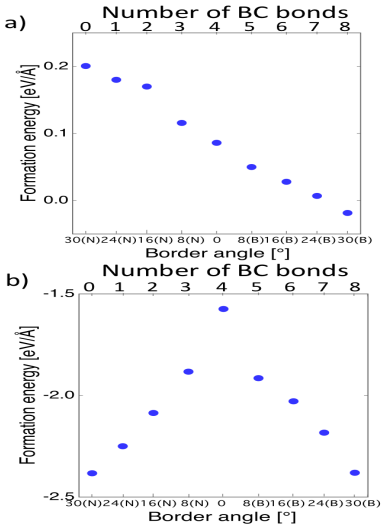

Fig. 5. The formation energy per unit length of border between h-BN and graphene in their heterostructure as a function of the border angle. The formation energy is evaluated from the total energies of h-BN and graphene strips with the (a) hydrogenated and (b) clean edges. Border angles of θ(N) and θ(B)° indicate the border angle θ consisting dominantly NC and BC bonds, respectively. The angle $\theta = 0$ and 30° corresponds with the armchair and zigzag borders, respectively.

borders with NC and BC heterobonds are more stable than the chiral and armchair borders, indicating that the heterostructures of h-BN and graphene prefer the zigzag border irrespective of the heterobond species at the border, under the ultra-high vacuum condition.

In summary, we investigated the energetics and formation mechanism of the border between h-BN and graphene using the DFT with GGA and ESM method. Our calculations showed that the total energy of the border between h-BN and graphene has energy minima at the border angle of 8° where the BC heterobond is dominant, because of the competition between the energy gain upon the formation of BC heterobond and the energy loss arising from the polarity at the border. By simulating the first and second stages of the BN adsorption at the graphene edges, BN are preferentially adsorbed at the zigzag edge of graphene by forming BC heterobond. We also calculated the formation energy of border in the heterostructure by connecting h-BN and graphene strips. The zigzag border containing BC heterobond is preferentially synthesized under the hydrogen rich condition, while the zigzag borders with BC and NC heterobonds are energetically preferable under ultra-high vacuum condition. Our simulations agree well with the experimental results and give the microscopic mechanism of the formation of border in heterostructure consisting of h-BN and graphene.

Acknowledgements

This work was supported by JST-CREST Grant Numbers JPMJCR1532 and JPMJCR1715 from the Japan Science and Technology Agency, JSPS KAKENHI Grant Numbers JP17H01069, JP16H00898, and JP16H06331 from the Japan Society for the Promotion of Science, and the Joint Research Program on Zero-Emission Energy Research, Institute of Advanced Energy, Kyoto University. Part of the calculations was performed on an NEC SX-Ace at the Cybermedia Center at Osaka University and on an SGI ICE XA/UV at the Institute of Solid State Physics, The University of Tokyo.

References

1) K.S. Novoselov, A.K. Geim, S.V. Morozov, D. Jiang, Y. Zhang, S.V. Dubonos, I.V. Grigorieva and A.A. Firsov, Science bf 306, 666 (2004).
2) I. Forbeaux, J.-M. Themlin and J.-M. Debever, Phys. Rev. B **58**, 16396 (1998).
3) C. Berger, Z. Song, X. Li, X. Wu, N. Brown, C. Naud, D. Mayou, T. Li, J. Hass, A.N. Marchenkov, E.H. Conrad, P.N. First and W.A. de Heer, Science **312**, 1191 (2006).
4) G. S. Painter and D. E. Ellis, Phys. Rev. **1**, 4747 (1970).
5) F. Bassani and G.P. Parravicini, Nuovo Cimento B **50**, 95 (1967).
6) M. Posternak, A. Baldereschi, A. J. Freeman, E. Wimmer and M. Weinert, Phys. Rev. Lett. **50**, 761 (1983).
7) N. Hamada, S. Sawada and A. Oshiyama, Phys. Rev. Lett. **68**, 1579 (1992).
8) R. Saito, M. Fujita, M. S. Dresselhaus and G. Dresselhaus, Appl. Phys. Lett. **60**, 2204 (1992).
9) K. Tanaka, K. Okahara, M. Okada and T. Yamabe, Chem. Phys. Lett. **191**, 469 (1992).
10) M. Fujita, K. Wakabayashi, K. Nakada and K. Kusakabe, J. Phys. Soc. Jpn. **65**, 1920 (1996).
11) K. Nakada, M. Fujita, G. Dresselhaus and M. S. Dresselhaus, Phys. Rev. B **54**, 17954 (1996).
12) K. Wakabayashi, M. Fujita, H. Ajiki and M. Sigrist, Phys. Rev. B **59**, 8271 (1999).
13) Y. Miyamoto, K. Nakada and M. Fujita, Phys. Rev. B **59**, 9858 (1999).
14) J. Kouvetakis, T. Sasaki, C. Chen, R. Hagiwara, M. Lerner, K. M. Krishnan and N. Bartlett, Synth. Metals **34**, 1-7 (1989).
15) K. M. Krishnan, Appl. Phys. Lett. **58**, 1857-1859 (1991).
16) D. Tománek, R. M. Wentzcovitch, S. G. Louie and M. L. Cohen, Phys. Rev. B **31**, 3134-3136 (1988).
17) Y. Miyamoto, A. Rubio, S. G. Louie and M. L. Cohen, Phys. Rev. B **50**, 18360-18366 (1994).
18) H. Nozaki and S. Itoh, J. Phys. Chem. Solids **57**, 41-49 (1996).
19) M. Benkraouda, J. Surperco. **15**, 650-662 (2002).
20) A. Y. Liu, R. M. Wentzcovitch and M. L. Cohen, Phys. Rev. B **39** 1760-1765 (1989).

21) S. M. Kim, A. Hsu, P. T. Araujo, Y.-H. Lee, T. Palacios, M. Dresselhaus, J.-C. Idrobo, K. K. Kim and J. Kong, Nano Lett. **13**, 933-941 (2013).
22) J. Park, J. Lee, L. Liu, K. W. Clark, C. Durand, C. Park, B. G. Sumpter, A. P. Baddorf, A. Mohsin, M. Yoon, G. Gu and A.-P. Li, Nature Commun. **5**, 5403 (2014).
23) C. Tönshoff, M. Müller, T. Kar, F. Latteyer, T. Chassé, K. Eichele and H. F. Bettinger, Chem. Phys. Chem. **13**, 1173-1181 (2012).
24) C. Sánchez-Sánchez, S. Brüller, H. Sachdev, K. Müllen, M. Krieg, H. F. Bettinger, A. Nicolaï, V. Meunier, L. Talirz, R. Fasel and P. Ruffieux, ACS Nano **9**, 9228-9235 (2015).
25) T. Gao, X. Song, H. Du, Y. Nie, Y. Chen, Q. Ji, J. Sun, Y. Yang, Y. Zhang and Z. Liu, Nature Commun. **6** 6835 (2015).
26) L. Ci, L. Song, C. Jin, D. Jariwala, D. Wu, Y. Li, A. Srivastava, Z. F. Wang, K. Storr, L. Balicas, F. Liu and P. M. Ajayan, Nature Mater. **9**, 430-435 (2010).
27) Y. Gao, Y. Zhang, P. Chen, Y. Li, M. Liu, T. Gao, D. Ma, Y. Chen, Z. Cheng, X. Qiu, W. Duan and Z. Liu, Nano Lett. **13**, 3439-3443 (2013).
28) E. Maeda, Y. Miyata, H. Hibino, Y. Kobayashi, R. Kitaura and H. Shinohara, Appl. Phys. Express **10**, 055102 (2017).
29) S. Okada, M. Igami, K. Nakada and A. Oshiyama, Phys. Rev. B **62**, 9896-9899 (2000).
30) S. Okada and A. Oshiyama, Phys. Rev. Lett. **87**, 146803 (2001).
31) M. Maruyama, N.T. Cuong and S. Okada, J. Phys. Chem. C **116**, 7581–7586 (2012).
32) H. Sawahata, M. Maruyama, N. T. Cuong, H. Omachi and H. Shinohara and S. Okada, ChemPhysChem **19**, 237-242 (2018).
33) P. Hohenberg and W. Kohn, Phys. Rev. **136**, B864 (1964).
34) W. Kohn and L. J. Sham, Phys. Rev. **140**, A1144 (1965).
35) Y. Morikawa, K. Iwata, and K. Terakura, Appl. Surf. Sci. **169-170**, 11 (2001).
36) J. P. Perdew, K. Burke, and M. Ernzerhof, Phys. Rev. Lett. **77**, 3865 (1997).
37) J. P. Perdew, K. Burke, and M. Ernzerhof, Phys. Rev. Lett. **78**, 1396 (1997).
38) D. Vanderbilt, Phys. Rev. B **41**, 7892 (1990).
39) A. Yamanaka and S. Okada, Carbon **96**, 351-361 (2016).
40) A. Yamanaka and S. Okada, Sci. Rep. **6**, 30653 (2016).
41) M. Otani and O. Sugino, Phys. Rev. B **73**, 115407 (2006).